Lab on a Chip

PAPER

View Article Online
View Journal

Cite this: DOI: 10.1039/c5lc00462d

Rapid and sensitive detection of antibiotic resistance on a programmable digital microfluidic platform†

Sumit Kalsi,[ab] Martha Valiadi,[ab] Maria-Nefeli Tsaloglou,[ab] Lesley Parry-Jones,[d] Adrian Jacobs,[d] Rob Watson,[c] Carrie Turner,[c] Robert Amos,[d] Ben Hadwen,[d] Jonathan Buse,[d] Chris Brown,[d] Mark Sutton[c] and Hywel Morgan*[ab]

Received 22nd April 2015,
Accepted 10th June 2015

DOI: 10.1039/c5lc00462d

www.rsc.org/loc

The widespread dissemination of CTX-M extended spectrum β-lactamases among *Escherichia coli* bacteria, both in nosocomial and community environments, is a challenge for diagnostic bacteriology laboratories. We describe a rapid and sensitive detection system for analysis of DNA containing the $bla_{\text{CTX-M-15}}$ gene using isothermal DNA amplification by recombinase polymerase amplification (RPA) on a digital microfluidic platform; active matrix electrowetting-on-dielectric (AM-EWOD). The devices have 16 800 electrodes that can be independently controlled to perform multiple and simultaneous droplet operations. The device includes an in-built impedance sensor for real time droplet position and size detection, an on-chip thermistor for temperature sensing and an integrated heater for regulating the droplet temperature. Automatic dispensing of droplets (45 nL) from reservoir electrodes is demonstrated with a coefficient of variation (CV) in volume of approximately 2%. The RPA reaction is monitored in real-time using exonuclease fluorescent probes. Continuous mixing of droplets during DNA amplification significantly improves target DNA detection by at least 100 times compared to a benchtop assay, enabling the detection of target DNA over four-order-of-magnitude with a limit of detection of a single copy within ~15 minutes.

Introduction

Antibiotic resistance is a growing global threat to human health. The effectiveness of antibiotics is diminishing rapidly as pathogens evolve various antibiotic resistance mechanisms, potentially making even simple infections difficult to treat. The resistance of Enterobacteriacae to cephalosporins and carbapenems has been classed as a serious hazard in the USA where 26 000 cases were reported in 2013, causing 1700 deaths.[1] The production of extended spectrum β-lactamases (ESBLs) in Gram-negative bacteria is an example of rapidly spreading antibiotic resistance fuelled by the overuse of common antibiotics. Amongst the wide range of ESBL enzymes, the CTX-M enzyme family is the most prevalent globally, conferring resistance to key β-lactam antibiotics such as cefotaxime.[2–4] The gene family encoding CTX-M, $bla_{\text{CTX-M}}$, is found in conjugative plasmids where genes are flanked by insertion sequences that make them highly mobile and promote strong expression.[5,6] Therefore, $bla_{\text{CTX-M}}$ have spread rapidly across at least 26 bacterial species residing in both nosocomial and community environments.[4] Of the CTX-M family, CTX-M-15, encoded by $bla_{\text{CTX-M-15}}$, is currently the most prevalent within the UK.

There is a clear need to develop rapid and sensitive tests to determine antibiotic resistance, both as part of the diagnosis and management of infection and to provide a rational basis for the appropriate prescription of antibiotics. This will allow for treatment with appropriate antibiotics to which the pathogens are sensitive, ensuring effective treatment of the patient's infection while preventing the development of further antibiotic resistance in the pathogen. Current clinical tests to detect antibiotic resistant bacteria are based on traditional bacterial cell culture, or on PCR based approaches that are lab based and require expert users and specialized equipment. In both cases, the analysis cannot be done near-patient, thereby delaying commencement of the appropriate treatment or resulting in the over-use of broad spectrum antibiotics.

The development of rapid, portable point-of-care tests for immediate diagnosis is now a major field of biomedical

[a] Electronics and Computer Science, University of Southampton, Southampton, SO17 1BJ, UK. E-mail: hm@ecs.soton.ac.uk
[b] Institute for Life Sciences, University of Southampton, Southampton, SO17 1BJ, UK
[c] Microbiology Services Division, Public Health England, Porton Down, Salisbury, SP4 0JG, UK
[d] Sharp Laboratories of Europe, Edmund Halley Road, Oxford Science Park, Oxford, OX4 4GB, UK

† Electronic supplementary information (ESI) available. See DOI: 10.1039/c5lc00462d

research.[7] The most rapid, sensitive and specific molecular assays are based on nucleic acid amplification to detect specific genes of interest, for example those that encode for ESBLs. Although PCR has been widely used in microsystems,[8–11] the advent of new isothermal DNA amplification techniques is ideal for point-of-care tests because thermal cycling equipment is not required, greatly simplifying the technology. Several isothermal amplification methods have been developed to target either RNA or DNA reviewed by Craw and Balachandran.[12] Rolling circle amplification (RCA),[13–15] loop mediated isothermal amplification (LAMP) *e.g.*[16–18] and helicase dependent amplification (HDA)[17,19] have all been used for the amplification of DNA in several microfluidic based assays. However, both LAMP and HDA methods require a high incubation temperature, which results in higher energy consumption and the branching primer pairs in RCA often lead to unspecific background amplification.[15] Additionally, with LAMP, the design of primers for a specific target is often limited by the need for 4 to 6 suitable primers over a small genomic region and the structure of the amplicon precludes verification of its identity. Recombinase polymerase amplification (RPA) has the advantage of being a highly sensitive rapid amplification method that proceeds at a relatively low temperature, is suitable for use on simple diagnostic devices, and is capable of detecting as few as 4 gene copies within 7 minutes.[20,21] Furthermore, the reaction can be easily monitored in real time by the use of a gene specific fluorescently labelled probe, which additionally makes the amplification process quantitative. Moreover, the reactions are less prone to inhibition by sample components than PCR and other amplification techniques, simplifying sample preparation.[22,23] These features make RPA an ideal candidate for rapid and field compatible diagnostic platforms which allow for real-time monitoring of the assay results.

Microfluidic devices represent a significant advancement for point-of-care tests and various chip designs have been developed in the quest for a fast molecular diagnostics platform. Most standard platforms for miniaturized nucleic acid extraction and amplification utilize (plastic) chips with compartments or channels through which reagents are pumped using a series of electrically controlled pumps and valves.[24–27] More recently, centrifugal forces have been used to control reagent flow in a 'lab-on-a-disc' device capable of extracting and amplifying DNA.[8,9,28–30] DNA amplification has also been carried out using the Slip Chip platform.[31,32]

Digital microfluidic micro-devices provide an alternative platform for miniaturised, fully automated assays, providing the basis of simple, programmable and portable test systems.[15,33–47] Based on the phenomenon of electrowetting-on-dielectric (EWOD), droplets with a wide range of volumes (microliter to sub-nL) can be individually manipulated using forces generated by an array of microelectrodes. EWOD-based chips (also known as digital microfluidics) have been used to perform molecular assays such as detection of single nucleotide polymorphisms,[48] DNA amplification,[15,49–51] immunoassays[52–55] and automated library preparation for next generation sequencing.[56] EWOD devices require very small volumes of reagent and manipulate and process precise droplet volumes, improving the assay performance (reviewed by Shen *et al.*[57]). Traditional "passive" EWOD devices are limited in their utility and are not programmable or reconfigurable owing to the number of independently programmable electrodes that can be operated on a single device. The recent development of EWOD devices controlled by Thin Film Transistor (TFT) electronics, so-called Active Matrix AM-EWOD, has overcome this problem.[34] The devices have large two-dimensional arrays of individually programmable electrodes facilitating the simultaneous and independent manipulation of many droplets in 2-dimension and giving a high level of flexibility in defining droplet size and shape. The AM-EWOD device also incorporates a TFT-based droplet sensing function to monitor the volume and position of droplets providing unique all-electronic control and monitoring of the assay. AM-EWOD devices are, therefore, ideally suited for point-of-care molecular testing as they provide a highly flexible and customisable platform capable of performing complex fluid manipulation of nanolitre volumes. These devices will be low cost, commensurate with the manufacturing cost of smartphone displays, and disposable.

In this paper we describe the application of AM-EWOD technology for a rapid and sensitive assay for the quantitative detection of the $bla_{\text{CTX-M-15}}$ antimicrobial resistance gene using an isothermal RPA reaction with fluorescence readout. We demonstrate the utility of this assay for highly sensitive detection of the gene, detecting fewer than 10 copies within 15 minutes and providing a hundred-fold improvement in the detection limit compared to an equivalent bench top assay.

Methods

1. Design of the AM-EWOD TFT backplane

The TFT backplane of the device is shown in Fig. 1 (photograph and diagram) and comprises an Active Matrix array of 96 × 175 TFT circuit elements. Each element has an associated ITO electrode of size 200 μm × 200 μm and adjacent electrodes are separated by a gap of 10 μm giving a total active area of the array of 7.37 cm^2. Each array element (see enlarged image in Fig. 1(a)) contains a TFT circuit to supply a voltage signal to the associated electrode which implements the electro-wetting actuation of droplets. Immediately adjacent to the high resolution array are nine fluid input structures, each comprising reservoir electrodes forming a path onto the main array. The electrodes for the fluid input structures are formed in the same ITO layer as used to form the electrodes in the main array and are controlled by the TFT circuitry in the same way as the main array. The design of the fluid input structure is shown in Fig. 1(b). It consists of a set of 7 electrodes with a total size of 3 mm × 9 mm for the purpose of dispensing and transferring fluid from the input reservoir electrodes onto the main part of the array. There are six fluid input structures along the long *x*-axis and three

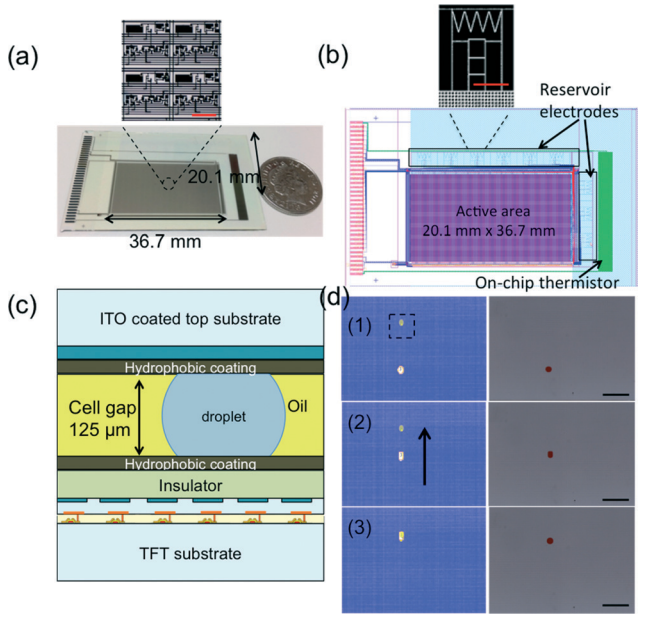

Fig. 1 (a) Photograph of the TFT backplane with an active matrix array of 96 × 175 TFT circuit elements within an area of 36.7 mm × 20.1 mm. A magnified image of four of the array elements is also shown. Scale bar: 100 μm. (b) Schematic diagram of the TFT backplane showing the nine reservoir electrodes, together with thermistor around the active area of array elements. The large reservoir electrodes were used to dispense daughter droplets onto the main array. Scale bar: 2 mm. (c) Schematic of cross section through the array, showing ITO coated top substrate and the individual transistors (not to scale). (d) Sequence of sensor output images together with optical images, showing the movement of a droplet from one position to another. The droplet (at the bottom) is first selected with a mouse click on the sensor output screen (1). The destination is then clicked on the same screen (shown by dotted box) to move the droplet (3). The software controls the direction and velocity of the droplet. Black arrow shows the direction of droplet movement (scale bar: 5 mm).

along the *y*-axis,. Electro-wetting actuation is controlled by an AC driving method as described in.[34] Each electrode is programmed to be in an actuated or non-actuated state with the programmed data being stored in a memory circuit within the array element. Row and column driver circuits and level shifter circuits are integrated onto the TFT substrate to control array addressing so that patterns of actuation data may be programmed to the device through a 5 V serial interface. The EWOD actuation voltage is 20 V.

Each array element also contains a sensor function for measuring capacitance, as previously described in.[34] The analogue sensor is used to detect the presence, partial presence or absence of liquid droplets present at the electrode. Row addressing and column readout amplifiers arrange for the measured sensor data to be output from the device as a serialised voltage signal. Thus a sensor image, showing the size and positions of the droplets upon the array is generated. Droplets may occupy single or multiple electrodes and image processing techniques have been developed to measure the size of the droplets from the output sensor image, as described in.[34] The actuation pattern can be re-written 50 times per second and a sensor image obtained 30 times per second. The sensor thus facilitates real time feedback of droplet size and position. A temperature sensor, comprising a metal thermistor (shown in Fig. 1(b)), is also integrated onto the TFT substrate to facilitate temperature measurement in proximity to the fluids.

2. Fabrication of the AM-EWOD TFT backplane

The Sharp CG Silicon TFT manufacturing process was used to fabricate the thin film electronics layers up to and including the ITO electrodes. The standard process used is identical to that used to fabricate small and medium sized displays, *e.g.* for mobile phones. Two additional layers were then added, (1) an ion barrier insulator, consisting of a 300 nm thick layer of Al_2O_3 deposited by Atomic Layer Deposition (ALD) and (2) a hydrophobic top coat generated by spin coating a layer of Cytop (Asahi Glass, Japan) of thickness approximately 80 nm. This Cytop coating was stripped and replaced for each new DNA assay.

3. Control electronics and software

A Printed Circuit Board (PCB) was custom designed to supply the voltage supplies and timing signals to drive the TFT electronics. Control firmware (VHDL) and application software (C#) was also custom designed to make the automated control of droplets easy to implement by the user. A set of droplet operations including move, merge, split, dispense and mix may be implemented by software control through a custom designed Graphical User Interface. Sequences of droplet operations may be pre-programmed by the user and implemented with real time feedback from the sensor. Alternatively droplets can be manipulated through 'click and drag' operations on the sensor image (see Fig. 1(d)).

The complete AM-EWOD device consists of the TFT backplane and a top substrate electrode which is also coated with Cytop. The two glass substrates are separated by a spacer whose height may be varied but is typically 125 μm. The droplets are manipulated in the space between the substrates within a filler medium of *n*-Dodecane. Fig. 1(c) shows a schematic diagram of a cross section of the assembled AM-EWOD device (not to scale). The top substrate electrode is fabricated from ITO and is completely transparent. The TFT backplane is partly transparent so that the overall transparency of the device is approximately 50%.

4. Integrated device heater

The RPA reaction requires the temperature to be controlled at approximately 39 °C. A novel method of heating the droplets was used to do this using a new design of top substrate electrode that functions as both the reference electrode and as a Joule heater. Strips along each end of the top substrate electrode were coated with aluminium to ensure a low resistance contact. One contact to the reference electrode is connected to an AC voltage signal for electro-wetting actuation. The other contact is connected *via* a low resistance

control switch so as either to be floating (no heating mode) or grounded (heating mode). The temperature was regulated by turning on and off the control switch and a Proportional Integral-Derivative (PID) control system (Omega, USA) was used to implement this, using the temperature measured by the glass thermistor. The total resistance of the top substrate electrode (comprised of a thin film of ITO) is approximately 100 ohms and the power dissipated by the heater (when in heating mode) is 4 W. The accuracy of the temperature was validated using a thermocouple placed within the cell gap. Temperature accuracy and uniformity across the device were evaluated using a thermo-chromic sheet (LCR Hallcrest Ltd, UK) with an accuracy of ±1 °C placed on the top plate. Measurements demonstrated that the temperature at the surface of the device could be heated to 39 °C (from room temperature) within 40 seconds and is maintained with a precision of better than ±1 °C across the area of the device.

5. DNA extraction from bacteria containing $bla_{\text{CTX-M-15}}$

DNA from an overnight culture of *E. coli* NCTC 13441 was extracted using the DNeasy Blood and Tissue Kit (Qiagen, UK) following the bacterial extraction protocol as described by the manufacturer. Eluted nucleic acid was quantified on a Qubit® fluorometer using DNA assay reagents. Genome copies were calculated from the DNA concentration using an in-house copy number calculator, although many are freely available online. The extracted DNA was then used for benchtop and EWOD RPA assay.

6. Primer design

Thirty-one primers spanning the $bla_{\text{CTX-M-15}}$ gene were designed and tested in multiple combinations using the TwistAmp Basic kit (TwistDx, UK) to identify the most efficient primer pair. Subsequently, RPA exo probes containing a Cy5 fluorophore were designed and evaluated using the TwistAmp exo kit (TwistDx, UK). The best performing primer pair/probe combination was used for the assay. The sequences for the primers and probes used in the study are available on request from Public Health England.

7. Benchtop Recombinase Polymerase Amplification (RPA)

RPA is an isothermal method of amplifying DNA with a recombinase ATPase, RecA. This forms complexes with two primers specific to the target gene that scans the DNA for complementary sequences.[58] A T4 polymerase, Bsu,[59] extends the primers, resulting in two copies of the original DNA. The amplification is monitored in real time using fluorescence; probes labelled with a tetrahydrofuran (THF) moiety that are complementary to the amplified DNA fragment. An exonuclease III included in the RPA reaction-mix digests the THF spacer when the probe is hybridised to the DNA resulting in the generation of fluorescence (see Fig. 2). The amplitude of the fluorescence signal is proportional to the amount of amplicon produced in the RPA reaction.

For the optimization process, benchtop RPA was performed using the TwistAmp Basic kit (TwistDx, UK) for end-point product visualisation, reactions were performed following the manufacturer's protocols. Briefly, lyophilised RPA proteins were reconstituted with a mix comprising rehydration solution, forward and reverse primers and sample. In each 50 μL reaction, final concentrations of primers were 0.48 μM. The RPA reaction mix was transferred to 0.2 mL PCR tubes and magnesium acetate added to a final concentration of 14 mM to initiate the reaction. Tubes were briefly centrifuged and immediately transferred to Veriti® thermal

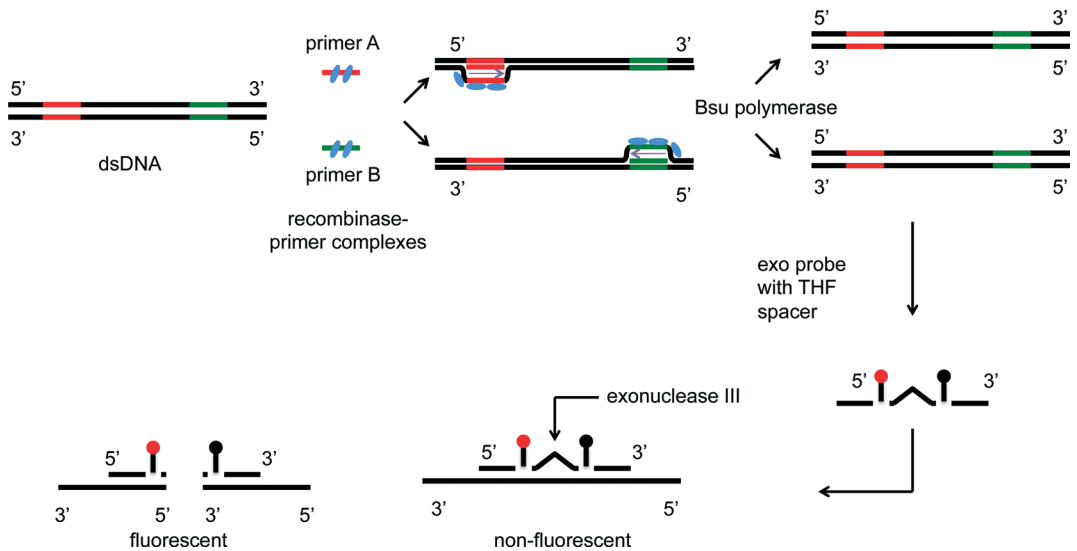

Fig. 2 Illustration of steps involved in the RPA reaction with real-time exo-nuclease probes. Double stranded DNA hybridizes with Recombinase-primer complexes. Primers are extended by polymerase to double the initial copy number. The exo-probe anneals to the complementary sequence on the template DNA. When the probe binds, exonuclease III digests the THF spacer causing real time fluorescence generation (adapted from ref. 21).

cycler (Applied Biosystems®, USA) for 60 minutes at 39 °C. Products were purified using a QIAquick PCR purification kit (Qiagen, UK) before visualising on a 1% agarose-TAE gel.

For the real-time reactions, RPA was performed using the TwistAmp Exo kit. The contents of the RPA reaction mix were identical except for a lower concentration of primers 0.42 μM and the addition of Cy5 labelled probe (0.12 μM). Following the addition of magnesium acetate, the reactions were mixed and the tubes were transferred to a BioRad Chromo 4 Real-Time Detector (qRT-PCR thermal cycler) where the fluorescence of the reaction was measured every 15 seconds for 60 minutes at 39 °C.

8. AM-EWOD device assembly and setup

For real-time RPA assay on AM-EWOD, master droplets of reagents and sample were loaded onto the AM-EWOD device by direct pipetting onto the reservoir electrodes (see Fig. 3(a)). The top substrate electrode was separated from the TFT backplane using Mylar spacers and the arrangement clamped to provide a well-defined cell gap (125 ± 1 μm) between the top plate and the TFT backplane. Fig. 1(c) shows a schematic diagram of a cross section of the assembled AM-EWOD device (not to scale). Each reservoir electrode was then actuated by turning on the appropriate voltage to immobilise the droplets onto the surface whilst the gap between top substrate and the TFT backplane was filled with dodecane. The device is then ready to manipulate droplets.

As a first step in the protocol, the required number and volume of droplets were dispensed from the input reservoirs. The size of each daughter droplet was defined by the number of activated elements. With an element size of 210 μm, and a 125 μm cell gap, a single element corresponded to a volume of approximately 5 nL. As is well known in EWOD technology,[60] the minimum size of droplet that can be created by splitting has a diameter of approximately 3–4 times the cell gap, so that with our choice of cell gap the minimum droplet size has a diameter of around 3 array elements. Smaller droplets could be created if desired by assembling the device with thinner spacers to form a smaller cell gap. A droplet was dispensed by turning off the reservoir electrodes and sequentially activating array elements in a direction perpendicular to the edge to form a "neck" of fluid. This "neck" was then broken by turning on the reservoir electrodes, creating a daughter droplet (Video S1, ESI†). The impedance sensor in each electrode detects the presence, location, size and shape of the droplets and provides active feedback to the software so that the appropriate array elements are actuated during this process.

Fluorescence generated by the molecular probe (labelled with Cy5) during DNA amplification was measured with a custom fluorescence detection system, described in.[31] This

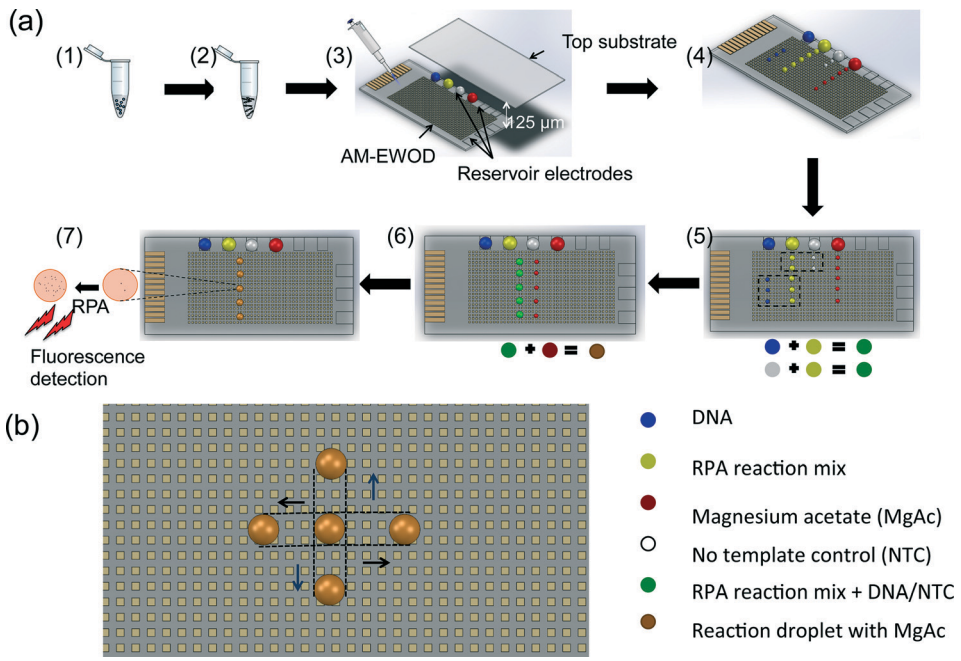

Fig. 3 (a) Schematic representation of the protocol for implementing the RPA assay on AM-EWOD device. An *E.coli* suspension is prepared (1), from which DNA containing $bla_{CTX\text{-}M\text{-}15}$ (2) is extracted. DNA sample, RPA reaction mix, magnesium acetate and no template control (NTC) is pipetted onto individual reservoir electrodes (3). Daughter droplets are dispensed from the reagent reservoirs (4). DNA and NTC is mixed with dispensed RPA reaction mix daughter droplets (5) and DNA-RPA reaction mix droplets are moved to the fluorescence detection position on EWOD (6). Magnesium acetate is mixed with the DNA-RPA reaction mix droplets to initiate the RPA reaction and the device heated to 39 °C (7). Real-time fluorescence is measured using custom-made optical setup, while continuously mixing the reaction droplets. (b) Schematic diagram showing mixing of a single droplet. The droplets are shuttled back and forth along the dotted lines, first along the *x*-axis, and then the *y*-axis. Observations showed that this produced excellent mixing whilst keeping the droplet centred in the field of view of the microscope objective on the optical system for fluorescence measurement.

setup measures fluorescence from each RPA reaction droplet at an excitation wavelength of 635 nm and emission of 692 nm. Each reaction droplet was imaged sequentially using a linear translation stage. The emitted fluorescence from the Cy5 probe was recorded during a 15 ms period to reduce photobleaching. The fluorescence was recorded for approximately 40 minutes and a total of 100 data points were recorded for each reaction droplet for the assay duration. The optical analysis software used was custom developed using LABVIEW™.

9. Real time RPA assays on AM-EWOD

The volumes of the different reagents for the RPA reaction were tailored for implementation in droplet format on the AM-EWOD microfluidic device. Tween® 20 (molecular biology grade, Sigma Aldrich, UK) was added to all the reagents to a final concentration of 0.1% v/v to reduce the surface tension of the droplets. The volume ratios were set to 4 : 1 : 1 for the RPA reaction mix, sample and magnesium acetate, respectively. The RPA reaction mix (RPA proteins, rehydration solution, primers and probe) was prepared so that the final assay component concentrations in the reaction droplet were identical to those in the 50 μL benchtop assay.

The complete protocol for the RPA assay on AM-EWOD is outlined in Fig. 3(a) (and Video S1, ESI†). The assay was repeated at two different volume scales, in each case preserving the same ratios. After dispensing the reagent and DNA containing droplets, the final reaction droplet volume was either 270 nL or 750 nL. For experiments using 270 nL reaction droplets, the four separate reservoir electrodes were loaded with droplets of RPA reaction mix, DNA (sample), nuclease free water (no template control, NTC) and magnesium acetate, each with approximate volumes of 2 μL. Daughter droplets (5× RPA reaction mix, 5× magnesium acetate, 3× DNA droplets and 2× NTC droplets) were then dispensed from the reservoir electrodes with the following volumes: RPA reaction mix = 180 nL (6 × 6 elements); DNA, NTC and magnesium acetate = 45 nL (3 × 3 elements). For experiments with 750 nL reaction droplets, five separate droplets were pipetted onto the active area of the device (see Fig. S1, ESI†) with the following volumes: 2.2 μL of magnesium acetate, 1.2 μL of DNA and NTC. Two separate RPA reaction mix droplets were used (3.2 μL and 2.2 μL), one for mixing with sample DNA and the other with NTC. Daughter droplets (500 nL, 10 × 10 elements for RPA and 125 nL, 5 × 5 elements for all others) were dispensed from the large droplets. The assay was not attempted with droplets smaller than 3 × 3 elements. However, by assembling a device with a 50 μm cell gap it was possible to demonstrate the manipulation of smaller droplets and the splitting of a droplet to a single element size (approximate volume of 2 nL).

After dispensing, the daughter droplets were moved to pre-determined regions on the array under direct software control (step (4), Fig. 3(a)). Reagent and sample droplets were mixed using a programmed mixing sequence (step (5) & (6), Fig. 3(a)), which repeatedly shuttles the droplets back and forth to achieve multiple folding of streamlines, considerably shortening the mixing time (see Video S1, ESI†). During mixing, the droplets had an approximately rectangular shape. Active mixing on EWOD reduced the time for mixing a 45 nL droplet with a 180 nL RPA reaction mix droplet to a minute compared to >40 min by passive mixing (diffusion). To quantify mixing, two 25 nL droplets containing dye (food colour) were merged with two 180 nL droplets of RPA reaction mix (which is viscous). In one droplet, active mixing was performed while the other was allowed to mix by diffusion. The distribution of dye within droplets was measured from the intensity of pixels in the recorded images. Images at the start of the mixing cycle (sampled every 1 minute) were compared with the images of the mixed droplet obtained at the end of the active mixing protocol and the two images subtracted. A histogram of the difference in the images gives information about the percentage of the droplet mixed.[61] An arbitrary threshold equal to a mean gray value of 5 was used to identify complete mixing. After 40 minutes, the mean gray value of the droplet with no active mixing was 6.8 ± 5.7 while the one with active mixing had a mean gray value of 4.1 ± 3.1 after only 1 minute.

The RPA reaction droplets were first mixed with the DNA (or NTC) (step 5) then with magnesium acetate (step 6) by moving the droplets a distance of ~3 mm or 600 μm from the centre position. The array was then heated to 39 °C using the integrated top plate heater to initiate the RPA reaction. During amplification, droplets were continuously mixed using a shuttling sequence (Fig. 3(b)). Other mixing methods could have been used such as extending the droplets along orthogonal axes, but this method was chosen to ensure that the droplets always remained within the field of view of the imaging objective. For continuous active mixing, droplets were moved a distance of approximately 600 μm from the laser spot.

10. Data analysis

The rate of generation of the target nucleic acid sequence can be quantified (as for PCR) by measuring the fluorescence signal as a function of time and determining the onset of amplification, or Time to Positivity (TTP).[21,62] To calculate this value, the background fluorescence for each duplicate (AM-EWOD) or triplicate (benchtop) negative control was averaged within a single assay and the standard deviation calculated. A threshold value of fluorescence was defined as a signal change equal to 3× the standard deviation of the negative control. The average fluorescence for all three droplets was determined and the TTP defined as the time taken for the fluorescence signal to cross this threshold value.

Results and discussion

1. Droplet dispensing on AM-EWOD

The reproducibility of the electronically dispensed droplet volumes was evaluated. This is important since any variation in the relative volumes of the sample and/or reagents may cause a corresponding variation in the measured optical

signal. We found that the reproducibility and accuracy of droplet dispensing depends on a number of factors, including the viscosity of the fluid and the size of the reservoir. Although the RPA reaction mix contains large molecular weight (Mw) polyethylene glycol (PEG) molecules and is quite viscous, all normal droplet operations such as merging, mixing, moving and splitting could be performed accurately and reliably using electro-wetting control.

For a fixed cell gap the droplet volume depends only on area, so that the size of each dispensed daughter droplet could be measured using the integrated impedance sensor. As has been shown previously,[34] this provides a highly accurate method of measurement the droplet volume. To characterise the dispensing protocols from the reservoir electrodes, droplets were dispensed using different variants of actuation patterns (as programmed by the software). The volumes of the dispensed droplets were measured by the impedance sensor and compared to the volume associated with the dispensing pattern (programmed volume) used (5 nL per array element). As shown in Fig. 4(a), there is a clear relationship between the dispensed volume and the actuation pattern used. The plotted data shows the average measured volume for 15 separate droplets dispensing actions (droplet removed, then returned to the reservoir). For small volumes, the dispensing pattern volume and droplet volumes closely correspond, but for the larger dispensed volumes (>125 nL) a small offset is observed of approximately 8%. Physically this arises from some of the fluid formed within the "neck" flowing back into the reservoir when the neck breaks and reducing dispensed droplet volume. This offset is taken into account when determining the assay protocol to give the desired ratio of reagents and samples of the droplets participating in the reaction. Table S1, ESI† summarises the data shown in Fig. 4(a).

For a programmed volume of 45 nL, the volumes dispensed from three of the nine reservoirs electrodes on the same device are shown in Fig. 4(b) (droplet removed, then returned to the reservoir). This data is for 15 dispensing actions from three pads, showing excellent reproducibility with coefficient of variation (CV) in dispensed volume of

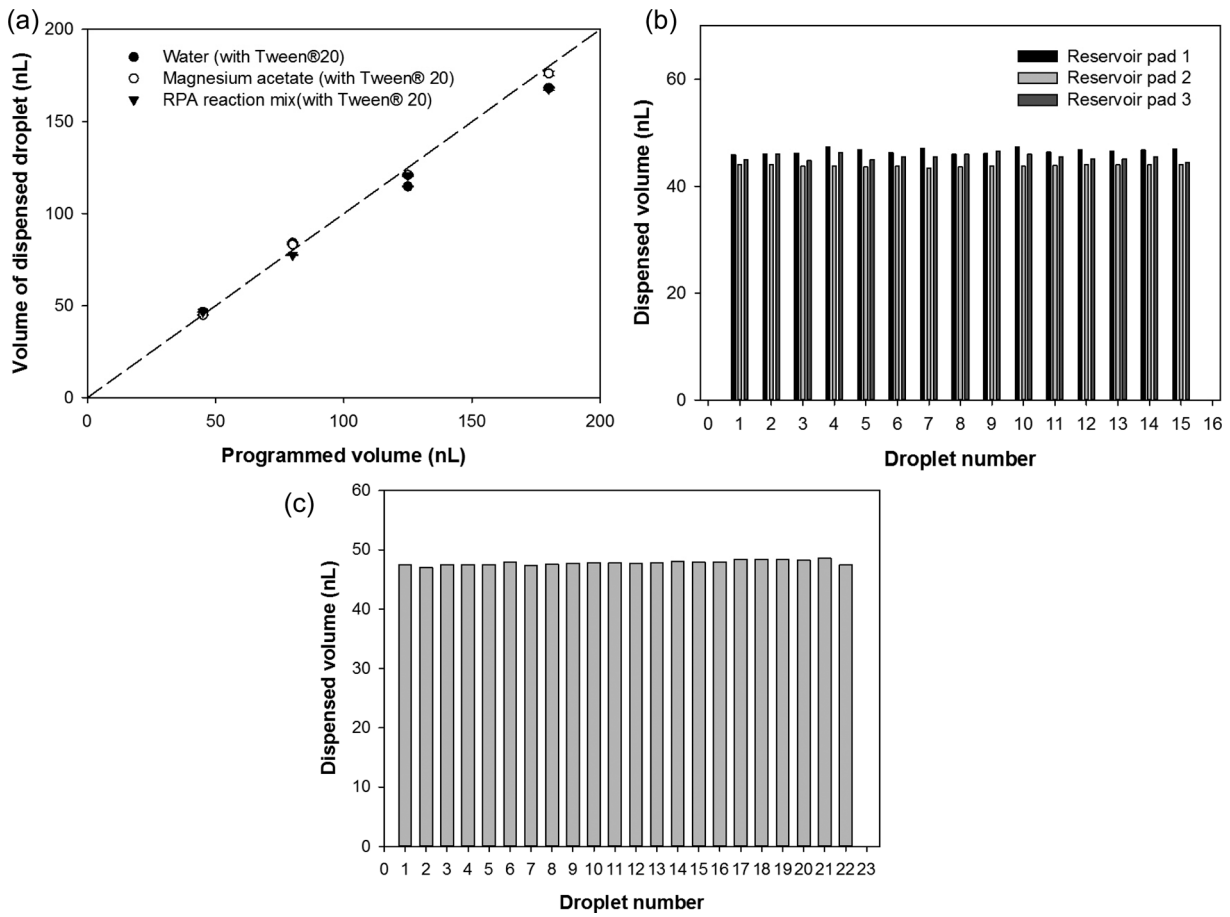

Fig. 4 (a) Comparison of programmed *vs.* actual dispensed volume of reagents. The dashed line shows the ideal case when the two volumes are equal. The data points is the average of 15 dispensed droplets (droplets removed and then returned to the reservoir). (b) Plot showing the volume (water with 0.1% Tween® 20) of 15 dispensed droplets from three of the reservoir pads (droplets removed and then returned to the reservoir). The programmed volume was set to 45 nL. (c) Volume of 22 consecutive droplets dispensed (water with 0.1% Tween® 20) from the reservoir pad (droplets removed and not returned to the reservoir). The programmed volume is 45 nL. The actual volume dispensed is calculated by multiplying the droplet area measured by the in-built impedance sensor by the cell gap height.

typically 1%. The device-to-device variation was also excellent, typically with a CV <1%. Fig. 4(c) shows the excellent repeatability in dispensing 22 consecutive 45 nL droplets from the reservoir electrodes (droplets not returned). A total cumulative volume of 1.05 μL could be withdrawn from a 2 μL reservoir volume with a CV in dispensed volume of 0.8% before large errors were introduced.

The accuracy in dispensing small droplets from large droplets placed directly onto the array was measured by withdrawing several 125 nL droplets from a much larger volume droplet (1.4 μL). A total of nine daughter droplets could be withdrawn (cumulative volume of 1.125 μL) with a volume CV of 4.8% (data not shown). This value is better than achievable by manual pipetting of small volumes, *e.g.* dispensing 0.2 μL with a 0.2–2 μL pipette has a typical CV of 20%.[63]

2. Bench-top RPA assay for CTX-M gene

The sensitivity of detection of the CTX-M gene using the RPA method was assessed by testing serial dilutions of genomic DNA extracted from clinical isolate *E. coli* 13441, with water used as a negative control. The amplification curves for a serial dilution of DNA performed using a qPCR machine (in triplicate) are shown in Fig. 5(a). The fluorescence intensity of the reaction increases exponentially after an initial lag phase with the signal saturating after 15 to 20 min. Time to positivity (TTP), defined as 3 times the standard deviation of the negative controls, increased with decreasing DNA concentration. A plot of TTP against logarithm of DNA concentration is shown in Fig. 5(d), with a linear relationship (R^2 = 0.919) for the RPA assay. This demonstrates the quantitative capability of the RPA assay. The limit of detection (LOD) for the benchtop assay is 5 pg genomic DNA, equivalent to 900 $bla_{\text{CTX-M-15}}$ copies, with a TTP of approximately 13 minutes.

3. DNA detection on AM-EWOD

To adapt the RPA assay for the EWOD platform, a surfactant (Tween® 20) was added to the RPA reagents. The purpose of the surfactant is to facilitate efficient low voltage droplet manipulation by lowering the surface tension. The effect of surfactant on the RPA assay was evaluated by performing a benchtop RPA assay with samples containing 0.1% v/v Tween®20. No difference in kinetics of the assay was

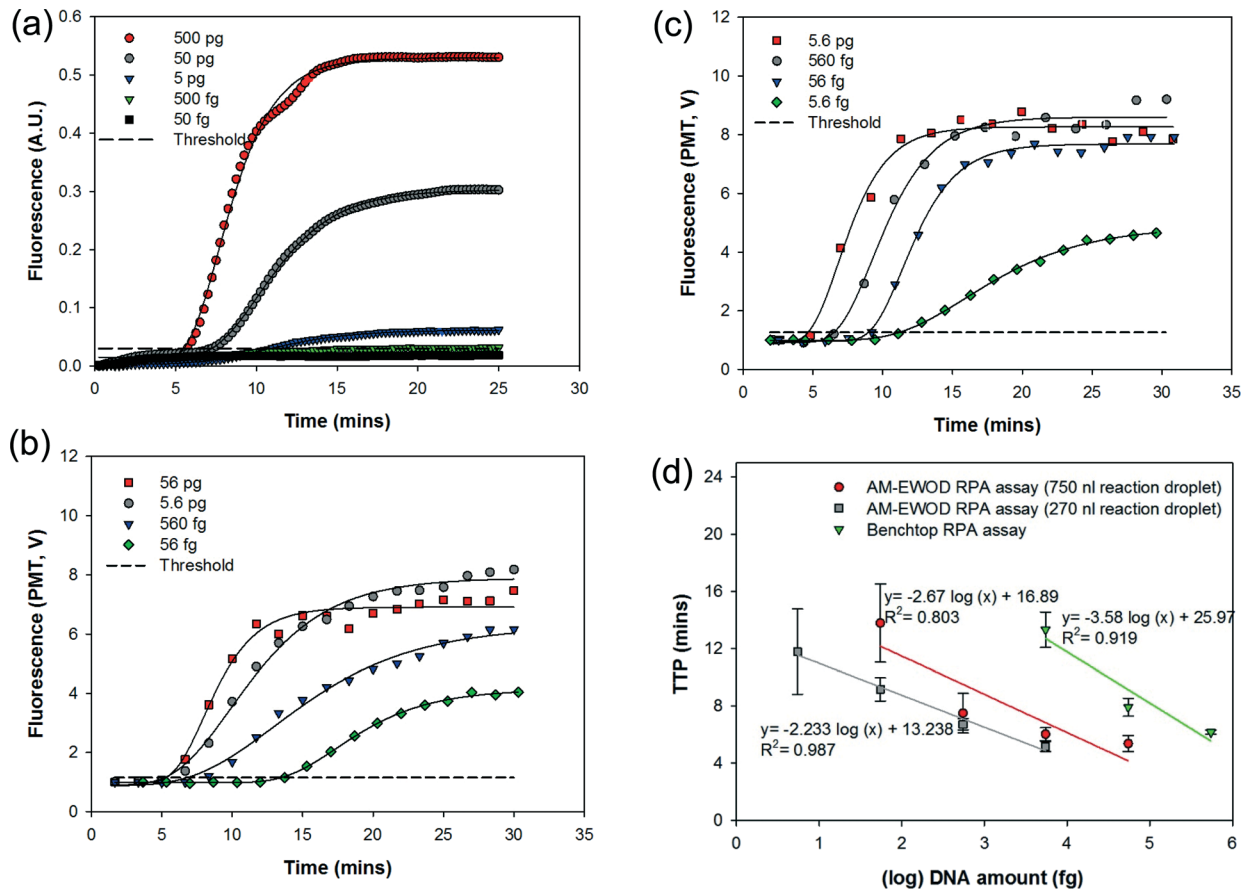

Fig. 5 RPA amplification curves of genomic DNA (with $bla_{\text{CTX-M-15}}$) extracted from clinical isolate *E.coli* 13441. (a) Average of triplicate RPA reactions for a given DNA concentration measured with a qPCR machine. (b & c) RPA reactions on AM-EWOD platform using (b) 750 nL reaction droplets and (c) 270 nL reaction droplets. Data is the average of three assays run simultaneously on the device. Dashed line defines the threshold specified as 3σ above the mean fluorescence of two negative control reactions (run together). Solid lines represent sigmoid fitted curves. (d) Plot of Time to Positivity (TTP) for the reactions shown) against logarithm of the amount of DNA (n = 3).

observed. We also established that the droplet microenvironment is well isolated from other droplets, *i.e.* there was no DNA contamination during manipulation, as evidenced by the consistent lack of amplification in the no template control (NTC) reactions.

Successful real-time amplification of $bla_{\text{CTX-M-15}}$ by RPA was demonstrated over a wide range of DNA concentrations (spanning four orders of magnitude) on the AM-EWOD device and repeated for the two reaction volumes used (750 nL and 270 nL) (Fig. 5(b and c)). The curves are the mean of the fluorescence signal from the three droplets and the data was obtained with a new (or a device stripped of Cytop and then re-coated) device for each DNA concentration. The relationship between TTP and logarithm of DNA is shown in Fig. 5(d) for both the 270 nL and 750 nL reaction droplets. As for the benchtop assays, the TTP decreased with increasing DNA concentration. The assays for the 750 nL and 270 nL droplets have similar sensitivities (slope of the fitted straight line in Fig. 5(d), but the TTP is shorter for the smaller droplet. This is probably due to faster mixing in the smaller droplets as a result of shorter diffusion paths. As the concentration of DNA is reduced, the standard deviation in the TTP increases. For the smaller droplet, the LOD is 5.6 fg (approximately a single copy), which is two orders of magnitude lower than the benchtop assay. Additionally, the TTP for any given DNA concentration is reduced by almost 50% compared to benchtop assay, which we attribute to the improved mixing on the AM-EWOD device. Unlike in the case of benchtop assay, the assay droplets on the device were continuously mixed during amplification. To explore the effect of continuous mixing on assay speed, the reaction was measured using two identical sets of droplets. In one set, all the reagents were mixed prior to heating the reaction but with no subsequent mixing. In the other set of droplets, the reaction mixture was continuously mixed. The results are shown in Fig. 6 for 1000 copies of DNA (5.6 pg DNA) and 270 nL reaction droplet. The effect of mixing on reaction kinetics is clear; the TTP has doubled for the unmixed samples, and the final fluorescence value is also much lower. These results demonstrate that continuous mixing significantly improves the assay performance and LoD on the AM-EWOD platform.

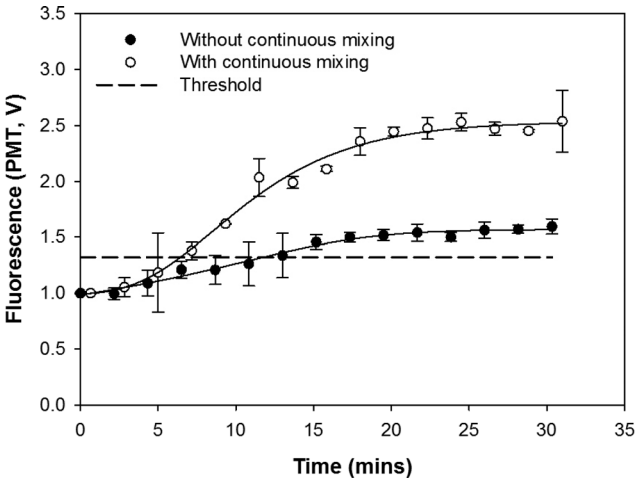

Fig. 6 Comparison of RPA amplification with and without continuous mixing on the AM-EWOD device. DNA concentration was 5.6 pg (with $bla_{\text{CTX-M-15}}$), approximately 1000 copies. The TTP is substantially reduced with continuous mixing of the reaction droplet, and the final signal is also significantly increased. Error bars denote the standard deviation for duplicate reactions. The dashed line defines the threshold and solid lines are fitted sigmoid curves.

Conclusion

This work has demonstrated the automated, rapid and sensitive detection of antibiotic resistance encoding genes using an isothermal DNA amplification method (RPA) with digital microfluidics on an AM-EWOD device.

Multiple and parallel droplet operations were performed on the device with the droplet handling protocol configured by software. We have demonstrated the dispensing of reagent and sample droplets of nanolitre volumes with excellent reproducibility of the generated volumes. The assay in droplet format uses very small volumes, reducing the consumption of reagents by more than 50 times compared to a conventional benchtop assay. Our results demonstrate single copy sensitivity with no problems from cross contamination. Positive amplification is obtained within 10 to 15 minutes, demonstrating the potential for a fast assay. The fast time-to-result was aided by an integrated heater/temperature sensing capability and the capability for fast droplet mixing on device. Assuming a consistent DNA extraction efficiency from bacterial samples and that 500 pg corresponds to 90 000 copies of the $bla_{\text{CTX-M-15}}$ gene with one copy per bacterium, the LoD is approximately a single organism.

We anticipate that the protocols developed here will form the basis for performing multiple assays on a single device. The large format and configurable nature of the AM-EWOD device is extremely well suited to scaling such that a single sample may be tested for multiple gene targets, simultaneously by the same device. It is expected that in future the technology will form the core of a rapid, disposable, and low cost point-of-care test for antibiotic resistance. By testing pathogens (isolated from patient samples) for the presence of multiple resistance genes, the clinician will be provided with the information necessary to prescribe an appropriate antibiotic. This will have significant benefits for patient outcomes (*i.e.* successful treatment of the infection) and for long term public health (*i.e.* avoiding the unnecessary use of broad spectrum antibiotics). One possible and example application is in the diagnosis and effective treatment of urinary tract infections (UTIs).

Contribution of authors

SK performed on-chip experiments, analysed the data and wrote the paper. MV did real-time benchtop RPA experiments. MNT performed intial RPA experiments and helped in

designing the probes. LPJ co-developed the assay protocols on device and the first proof of concept experiments on device. Contributed to the design and build of the measurement optics. AJ developed the coating methods for the glass chip. Contributed to the development of the assay protocols on device. JB designed and built the hardware and firmware for supplying voltages and timing signals to the glass chip and the thermal control system for integrated temperature control. RW and CT did benchtop assay experiments and molecular biology for the assay. RA designed and built the software for controlling droplet operations. First inventor of the method for temperature control on device. BH designed the glass chip electronics. Development of the method of on-chip heating and temperature feedback. CB managed the development team at SLE. Contributed to the design of the glass chip electronics. MS advised on microbiology work. HM managed the project, analysed data and wrote the paper.

Acknowledgements

This work has been supported by National Institute for Health Research (NIHR), Rapid detection of infectious agents at point of triage (PoT), II-ES-0511-21002. The views expressed in this publication are those of the author(s) and not necessarily those of the NHS, the National Institute for Health Research or the Department of Health. The authors are grateful to Dr Olaf Pipenburg (Twistdx, UK) for useful discussions. The authors would like to thank Sarah Helps for Cytop coating the TFT backplanes and top substrates, and Kai Ming Chang for support with microscope setup for optical imaging of droplets.

References

1 CDC, *Antibiotic resistance threats in the United States*, 2013, http://www.cdc.gov/drugresistance/threat-report-2013/, [Accessed 10/October/2014].
2 R. Bonnet, *Antimicrob. Agents Chemother.*, 2004, **48**, 1–14.
3 M. M. D'Andrea, F. Arena, L. Pallecchi and G. M. Rossolini, *Int. J. Med. Microbiol.*, 2013, **303**, 305–317.
4 W.-H. Zhao and Z.-Q. Hu, *Crit. Rev. Microbiol.*, 2013, **39**, 79–101.
5 L. Poirel, M.-F. Lartigue, J.-W. Decousser and P. Nordmann, *Antimicrob. Agents Chemother.*, 2005, **49**, 447–450.
6 L. Poirel, J.-W. Decousser and P. Nordmann, *Antimicrob. Agents Chemother.*, 2003, **47**, 2938–2945.
7 V. Gubala, L. F. Harris, A. J. Ricco, M. X. Tan and D. E. Williams, *Anal. Chem.*, 2012, **84**, 487–515.
8 J. G. Lee, K. H. Cheong, N. Huh, S. Kim, J. W. Choi and C. Ko, *Lab Chip*, 2006, **6**, 886–895.
9 Y. K. Cho, J. G. Lee, J. M. Park, B. S. Lee, Y. Lee and C. Ko, *Lab Chip*, 2007, **7**, 565–573.
10 H. Norian, R. M. Field, I. Kymissis and K. L. Shepard, *Lab Chip*, 2014, **14**, 4076–4084.
11 Z. Hua, J. L. Rouse, A. E. Eckhardt, V. Srinivasan, V. K. Pamula, W. A. Schell, J. L. Benton, T. G. Mitchell and M. G. Pollack, *Anal. Chem.*, 2010, **82**, 2310–2316.
12 P. Craw and W. Balachandran, *Lab Chip*, 2012, **12**, 2469–2486.
13 K. Sato, A. Tachihara, B. Renberg, K. Mawatari, K. Sato, Y. Tanaka, J. Jarvius, M. Nilsson and T. Kitamori, *Lab Chip*, 2010, **10**, 1262–1266.
14 J. Melin, H. Johansson, O. Soderberg, F. Nikolajeff, U. Landegren, M. Nilsson and J. Jarvius, *Anal. Chem.*, 2005, **77**, 7122–7130.
15 M. Kuhnemund, D. Witters, M. Nilsson and J. Lammertyn, *Lab Chip*, 2014, **14**, 2983–2992.
16 C.-H. Wang, K.-Y. Lien, J.-J. Wu and G.-B. Lee, *Lab Chip*, 2011, **11**, 1521–1531.
17 X. Fang, Y. Liu, J. Kong and X. Jiang, *Anal. Chem.*, 2010, **82**, 3002–3006.
18 D. Tourlousse, F. Ahmad, R. Stedtfeld, G. Seyrig, J. Tiedje and S. Hashsham, *Biomed. Microdevices*, 2012, **14**, 769–778.
19 S. Huang, J. Do, M. Mahalanabis, A. Fan, L. Zhao, L. Jepeal, S. K. Singh and C. M. Klapperich, *PLoS One*, 2013, 8.
20 X. Xia, Y. Yu, L. Hu, M. Weidmann, Y. Pan, S. Yan and Y. Wang, *Arch. Virol.*, 2015, **160**, 987–994.
21 O. Piepenburg, C. H. Williams, D. L. Stemple and N. A. Armes, *PLoS Biol.*, 2006, **4**, e204.
22 S. Santiago-Felipe, L. A. Tortajada-Genaro, S. Morais, R. Puchades and A. Maquieira, *Food Chem.*, 2015, **174**, 509–515.
23 K. Krolov, J. Frolova, O. Tudoran, J. Suhorutsenko, T. Lehto, H. Sibul, I. Mager, M. Laanpere, I. Tulp and U. Langel, *J. Mol. Diagn.*, 2014, **16**, 127–135.
24 Q. Cao, M. Mahalanabis, J. Chang, B. Carey, C. Hsieh, A. Stanley, C. A. Odell, P. Mitchell, J. Feldman, N. R. Pollock and C. M. Klapperich, *PLoS One*, 2012, 7.
25 L. Van Heirstraeten, P. Spang, C. Schwind, K. S. Drese, M. Ritzi-Lehnert, B. Nieto, M. Camps, B. Landgraf, F. Guasch, A. H. Corbera, J. Samitier, H. Goossens, S. Malhotra-Kumar and T. Roeser, *Lab Chip*, 2014, **14**, 1519–1526.
26 M. Mahalanabis, J. Do, H. Almuayad, J. Zhang and C. Klapperich, *Biomed. Microdevices*, 2010, **12**, 353–359.
27 C.-J. Liu, K.-Y. Lien, C.-Y. Weng, J.-W. Shin, T.-Y. Chang and G.-B. Lee, *Biomed. Microdevices*, 2009, **11**, 339–350.
28 T.-H. Kim, J. Park, C.-J. Kim and Y.-K. Cho, *Anal. Chem.*, 2014, **86**, 3841–3848.
29 L. A. Tortajada-Genaro, S. Santiago-Felipe, M. Amasia, A. Russom and A. Maquieira, *RSC Adv.*, 2015, **5**, 29987–29995.
30 S. Santiago-Felipe, L. A. Tortajada-Genaro, S. Morais, R. Puchades and Á. Maquieira, *Sens. Actuators, B*, 2014, **204**, 273–281.
31 M. N. Tsaloglou, R. J. Watson, C. M. Rushworth, Y. Zhao, X. Niu, J. M. Sutton and H. Morgan, *Analyst*, 2015, **140**, 258–264.
32 F. Shen, E. K. Davydova, W. Du, J. E. Kreutz, O. Piepenburg and R. F. Ismagilov, *Anal. Chem.*, 2011, **83**, 3533–3540.
33 M. J. Jebrail, A. Sinha, S. Vellucci, R. F. Renzi, C. Ambriz, C. Gondhalekar, J. S. Schoeniger, K. D. Patel and S. S. Branda, *Anal. Chem.*, 2014, **86**, 3856–3862.
34 B. Hadwen, G. R. Broder, D. Morganti, A. Jacobs, C. Brown, J. R. Hector, Y. Kubota and H. Morgan, *Lab Chip*, 2012, **12**, 3305–3313.

35 R. B. Fair, *Microfluid. Nanofluid.*, 2007, **3**, 245–281.
36 W. C. Nelson and C.-J. C. Kim, *J. Adhes. Sci. Technol.*, 2012, **26**, 1747–1771.
37 A. H. Ng, K. Choi, R. P. Luoma, J. M. Robinson and A. R. Wheeler, *Anal. Chem.*, 2012, **84**, 8805–8812.
38 D. Witters, N. Vergauwe, S. Vermeir, F. Ceyssens, S. Liekens, R. Puers and J. Lammertyn, *Lab Chip*, 2011, **11**, 2790–2794.
39 V. Nicolas, W. Daan, C. Frederik, V. Steven, V. Bert, P. Robert and L. Jeroen, *J. Micromech. Microeng.*, 2011, **21**, 054026.
40 N. Vergauwe, S. Vermeir, J. B. Wacker, F. Ceyssens, M. Cornaglia, R. Puers, M. A. M. Gijs, J. Lammertyn and D. Witters, *Sens. Actuators, B*, 2014, **196**, 282–291.
41 G. J. Shah, H. Ding, S. Sadeghi, S. Chen, C. J. Kim and R. M. van Dam, *Lab Chip*, 2013, **13**, 2785–2795.
42 W. C. Nelson, I. Peng, G. A. Lee, J. A. Loo, R. L. Garrell and C. J. Kim, *Anal. Chem.*, 2010, **82**, 9932–9937.
43 M. G. Pollack, R. B. Fair and A. D. Shenderov, *Appl. Phys. Lett.*, 2000, **77**, 1725–1726.
44 V. Srinivasan, V. K. Pamula and R. B. Fair, *Lab Chip*, 2004, **4**, 310–315.
45 R. B. Fair, A. Khlystov, T. D. Tailor, V. Ivanov, R. D. Evans, P. B. Griffin, S. Vijay, V. K. Pamula, M. G. Pollack and J. Zhou, *IEEE Des. Test Comput.*, 2007, **24**, 10–24.
46 S. K. Cho, H. Moon and K. Chang-Jin, *J. Microelectromech. Syst.*, 2003, **12**, 70–80.
47 E. M. Miller and A. R. Wheeler, *Anal. Chem.*, 2008, **80**, 1614–1619.
48 S. Hsien-Hua, S. Tsung-Yao, C. Hwan-You and Y. Da-Jeng, *IEEE Conference Nanotechnology Materials and Devices*, 2012, pp. 92–95.
49 A. Rival, D. Jary, C. Delattre, Y. Fouillet, G. Castellan, A. Bellemin-Comte and X. Gidrol, *Lab Chip*, 2014, **14**, 3739–3749.
50 K. Ugsornrat, T. Maturos, T. Pogfai, A. Wisitsoraat, T. Lomas and A. Tuantranont, *8th conference on electrical engineering/electronics, computer, telecommunications and information technology*, 2011, pp. 6–9.
51 M. J. Jebrail, H. Yang, J. M. Mudrik, N. M. Lafreniere, C. McRoberts, O. Y. Al-Dirbashi, L. Fisher, P. Chakraborty and A. R. Wheeler, *Lab Chip*, 2011, **11**, 3218–3224.
52 M.-N. Tsaloglou, A. Jacobs and H. Morgan, *Anal. Bioanal. Chem.*, 2014, **406**, 5967–5976.
53 L. Zhu, Y. Feng, X. Ye, J. Feng, Y. Wu and Z. Zhou, *J. Adhes. Sci. Technol.*, 2012, **26**, 2113–2124.
54 M. H. Shamsi, K. Choi, A. H. Ng and A. R. Wheeler, *Lab Chip*, 2014, **14**, 547–554.
55 K. Choi, A. H. Ng, R. Fobel, D. A. Chang-Yen, L. E. Yarnell, E. L. Pearson, C. M. Oleksak, A. T. Fischer, R. P. Luoma, J. M. Robinson, J. Audet and A. R. Wheeler, *Anal. Chem.*, 2013, **85**, 9638–9646.
56 Illumina, *Neoprep Library Prep System*, http://www.illumina.com/systems/neoprep-library-system.html [Accessed 28/May/2015].
57 H. H. Shen, S. K. Fan, C. J. Kim and D. J. Yao, *Microfluid. Nanofluid.*, 2014, **16**, 965–987.
58 T. Shibata, R. P. Cunningham, C. Dasgupta and C. M. Radding, *Proc. Natl. Acad. Sci. U. S. A.*, 1979, **76**, 5100–5104.
59 T. Okazaki and A. Kornberg, *J. Biol. Chem.*, 1964, **239**, 259–268.
60 H. Ding, S. Sadeghi, G. J. Shah, S. Chen, P. Y. Keng, C. J. Kim and R. M. van Dam, *Lab Chip*, 2012, **12**, 3331–3340.
61 P. Paik, V. K. Pamula and R. B. Fair, *Lab Chip*, 2003, **3**, 253–259.
62 M. Euler, Y. Wang, P. Otto, H. Tomaso, R. Escudero, P. Anda, F. T. Hufert and M. Weidmann, *J. Clin. Microbiol.*, 2012, **50**, 2234–2238.
63 Thermoscientific, *Good laboratory pipetting guide*, 2010, http://www.thermoscientific.com/finpipette [Accessed 5/November/2014].